

# EXPONENTIAL RADON TRANSFORM INVERSION BASED ON HARMONIC ANALYSIS OF THE EUCLIDEAN MOTION GROUP

Can Evren Yarman, Birsen Yazıcı

Rensselaer Polytechnic Institute,  
Electrical, Computer and System Engineering  
Troy, NY

## ABSTRACT

This paper presents a new method for the exponential Radon transform inversion based on harmonic analysis of the Euclidean motion group  $M(2)$ . The exponential Radon transform is modified to be formulated as a convolution over  $M(2)$ . The convolution representation leads to a block diagonalization of the modified exponential Radon transform in the Euclidean motion group Fourier domain, which provides a deconvolution type inversion for the exponential Radon transform. Numerical examples are presented to show the viability of the proposed method.

## 1. INTRODUCTION

For a uniform attenuation coefficient  $\mu \in \mathbb{C}$ , the exponential Radon transform of a compactly supported real valued function  $f$  over  $\mathbb{R}^2$  is defined as

$$\mathcal{T}_\mu f(\boldsymbol{\theta}, t) = \int_{\mathbb{R}^2} f(\mathbf{x}) \delta(\mathbf{x} \cdot \boldsymbol{\theta} - t) e^{\mu \mathbf{x} \cdot \boldsymbol{\theta}^\perp} d\mathbf{x}, \quad (1)$$

where  $t \in \mathbb{R}$ ,  $\boldsymbol{\theta} = (\cos \theta, \sin \theta)^T$  is a unit vector on  $S^1$  with  $\theta \in [0, 2\pi)$  and  $\boldsymbol{\theta}^\perp = (-\sin \theta, \cos \theta)^T$ .

The exponential Radon transform constitutes a mathematical model for imaging modalities such as x-ray tomography ( $\mu = 0$ ), single photon emission tomography (SPECT) ( $\mu \in \mathbb{R}$ ) [7], and optical polarization tomography of stress tensor field ( $\mu \in i\mathbb{R}$ ) [8].

A number of different approaches have been proposed for the exponential Radon transform inversion. These can be classified into three categories: Fourier, filtered back projection and circular harmonic decomposition [1, 9, 3, 2, 4, 6] type inversion methods. A unified framework and a detailed review of the inversion methods can be found in [6].

This paper presents an alternative approach and provides a new inversion method for the exponential Radon transform based on the harmonic analysis of the Euclidean motion group, denoted by  $M(2)$ . This method of inversion leads to new algorithms for the inversion of the exponential Radon transform. The reconstructed images for  $\mu$  real and  $\mu$  imaginary are presented to show the viability of the proposed method.

## 2. MODIFIED EXPONENTIAL RADON TRANSFORM AS A CONVOLUTION OVER THE GROUP $M(2)$

The rigid motions of  $\mathbb{R}^2$  form a group called the Euclidean motion group denoted by  $M(2)$ . The elements of the group are the  $3 \times 3$

dimensional matrices of the form

$$(R_\theta, \mathbf{r}) = \begin{bmatrix} R_\theta & \mathbf{r} \\ \mathbf{0}^T & 1 \end{bmatrix}, \quad (2)$$

where  $R_\theta = \begin{bmatrix} \cos \theta & -\sin \theta \\ \sin \theta & \cos \theta \end{bmatrix} \in SO(2)$  is the rotation component and  $\mathbf{r} = (r_1, r_2)^T \in \mathbb{R}^2$  is the translation component. The group operation is the usual matrix multiplications and inverse of an element is obtained by matrix inversion as  $(R_\theta, \mathbf{r})^{-1} = (R_\theta^{-1}, -R_\theta^{-1}\mathbf{r})$ .

Let  $g = (R_\theta, \mathbf{r})$  and  $h = (R_\phi, \mathbf{x})$ . Convolution over  $M(N)$  is defined as

$$(f_1 *_{M(2)} f_2)(g) = \int_{M(2)} f_1(h) f_2(h^{-1}g) d(h) \quad (3)$$

where  $\int_{M(2)} d(h) = \int_{SO(2)} \int_{\mathbb{R}^2} d\mathbf{x} d(\phi)$ . Then, multiplying the exponential Radon transform of a real valued function  $f$  with  $e^{\mu r_2}$ ,  $r_2 \in \mathbb{R}$ , the resulting integral can be expressed as a convolution operation over  $M(2)$  as follows:

$$\begin{aligned} \mathcal{T}'_\mu f(g) &= e^{\mu r_2} \mathcal{T}_\mu f(\boldsymbol{\vartheta}, -r_1) \\ &= \int_{\mathbb{R}^2} f(\mathbf{x}) \delta(\mathbf{x} \cdot \boldsymbol{\vartheta} + r_1) e^{\mu \mathbf{x} \cdot \boldsymbol{\vartheta}^\perp + \mu r_2} d\mathbf{x} \\ &= (\Lambda_\mu *_{M(2)} f^*)(g), \end{aligned} \quad (4)$$

where  $f^*(h) = \overline{f(h^{-1})}$  and  $\Lambda_\mu(h) = \delta(\mathbf{x} \cdot \mathbf{e}_1) e^{\mu \mathbf{x} \cdot \mathbf{e}_2}$ .  $\Lambda_\mu$  will be called the convolution filter.

We shall use the Fourier transform over the group  $M(2)$  to express the modified exponential Radon transform,  $\mathcal{T}'_\mu f$ , as a multiplication in the  $M(2)$ -Fourier domain.

## 3. $M(2)$ -FOURIER TRANSFORM

Let  $f \in L^2(M(2))$ . The  $M(2)$ -Fourier transform of  $f$  is defined as

$$\mathcal{F}_{M(2)}(f)_{mn}(\lambda) = \widehat{f}_{mn}(\lambda) = \int_{M(2)} f(g) u_{mn}^{(\lambda)}(g^{-1}) d(g), \quad (5)$$

for  $\lambda \geq 0$ , and the corresponding inverse  $M(2)$ -Fourier transform is given by

$$\mathcal{F}_{M(2)}^{-1}(\widehat{f}_{mn})(g) = f(g) = \int_0^\infty \sum_{m,n} \widehat{f}_{mn}(\lambda) u_{nm}^{(\lambda)}(g) \lambda d\lambda, \quad (6)$$

where  $u_{mn}^{(\lambda)}(g)$  are the matrix elements of the irreducible unitary representations of  $M(2)$  given by [10]

$$u_{mn}^{(\lambda)}(g) = \frac{1}{2\pi} \int_0^{2\pi} e^{-im\omega} e^{-i\lambda(r_1 \cos \omega + r_2 \sin \omega)} e^{in(\omega - \theta)} d\omega. \quad (7)$$

Let  $f, f_1, f_2 \in L^2(M(2))$ . Then,  $M(2)$ -Fourier transform satisfies the following properties:

1. Adjoint property:

$$\widehat{f^*}_{mn}(\lambda) = \overline{\widehat{f}_{nm}(\lambda)}, \quad (8)$$

where  $f^*(g) = \overline{f(g^{-1})}$ .

2. Convolution property:

$$\mathcal{F}(f_1 * f_2)_{mn}(\lambda) = \sum_q \widehat{f}_{2mq}(\lambda) \widehat{f}_{1qn}(\lambda). \quad (9)$$

3. If  $f$  is an  $SO(2)$  invariant function over  $M(2)$ , i.e.  $f(g) = f(\mathbf{r}) \in L^2(\mathbb{R}^2)$ , then

$$\widehat{f}_{mn}(\lambda) = \delta_m \widetilde{f}_n(-\lambda) \quad (10)$$

where  $\delta_m$  is the Kronecker delta function.

#### 4. INVERSION OF EXPONENTIAL RADON TRANSFORM USING $M(2)$ -FOURIER TRANSFORM

Treating the projections  $\mathcal{T}'f_\mu$  and the filter  $\Lambda_\mu$  as distributions over  $M(2)$ , the modified exponential Radon transform can be expressed as a multiplication in the  $M(2)$ -Fourier transform domain. Using the convolution property of the  $M(2)$ -Fourier transform, (4) becomes:

$$\widehat{\mathcal{T}'f}_{mn}(\lambda) = \sum_q \overline{\widehat{f}_{qm}(\lambda)} \widehat{\Lambda}_{\mu qn}(\lambda) = \overline{\widehat{f}_{0m}(\lambda)} \widehat{\Lambda}_{\mu 0n}(\lambda), \quad (11)$$

for  $m, n \in \mathbb{Z}$ . Equation 11 provides a block diagonal representation of the modified exponential Radon transform in the  $M(2)$ -Fourier domain, where each block is parameterized by  $\lambda \geq 0$ . It also provides an immediate inversion formula for the exponential Radon transform:

$$f = \mathcal{F}_{M(2)}^{-1} \left( \sum_k \left[ \widehat{\mathcal{T}'f}_{nk} \left[ \widehat{\Lambda}_\mu \right]_{km}^{-1} \right]^\dagger \right). \quad (12)$$

Since  $\widehat{\Lambda}_\mu$  is rank one, as long as  $\widehat{\Lambda}_{\mu 0n}(\lambda) \neq 0$ , by (11), the  $M(2)$ -Fourier coefficients of  $f$  is given by

$$\widehat{f}_{0m}(\lambda) = \left( \frac{\widehat{\mathcal{T}'f}_{mn}(\lambda)}{\widehat{\Lambda}_{\mu 0n}(\lambda)} \right). \quad (13)$$

Thus, the inversion formula for the exponential Radon transform becomes:

$$\begin{aligned} f(\mathbf{x}) &= \mathcal{F}_{M(2)}^{-1} \left( \delta_k \widetilde{f}_{-m}(-\lambda) \right) = \mathcal{F}^{-1} \left( \delta_k \left( \frac{\widehat{\mathcal{T}'f}_{mn}(\lambda)}{\widehat{\Lambda}_{\mu 0n}(\lambda)} \right) \right) \\ &= \int_0^\infty \sum_m \left( \frac{\widehat{\mathcal{T}'f}_{mn}(\lambda)}{\widehat{\Lambda}_{\mu 0n}(\lambda)} \right) u_{m0}^{(\lambda)}(h) \lambda^{N-1} d\lambda. \end{aligned} \quad (14)$$

#### 5. RECONSTRUCTION ALGORITHMS

Two algorithms are proposed for exponential Radon transform inversion. The algorithms differ mainly in the way the  $M(2)$ -Fourier coefficients,  $\widehat{f}_{0m}(\lambda)$ , of the function are computed (step 3 of the reconstruction). In the first algorithm, (14) is used to compute  $\widehat{f}_{0m}(\lambda)$ , whereas in the second algorithm, (12) is used. Let  $f(\mathbf{x}) = 0$  for  $|\mathbf{x}| > a$  and hence  $\mathcal{T}_\mu f(\theta, r_1) = 0$  for  $|r_1| > a$ . Proposed exponential Radon transform inversion can be implemented in four steps:

Step 1. Extend  $\mathcal{T}_\mu f(\theta, -r_1)$  to  $\mathcal{T}'_\mu f(g)$  by multiplying with  $e^{\mu r_2}$  for  $r_2 \in [-a, a]$ , where  $0 < a < \infty$ .

Step 2. Compute  $\widehat{\mathcal{T}'_\mu f}_{mn}(\lambda)$ , the  $M(2)$ -Fourier transform of  $\mathcal{T}'_\mu f$  for  $m, n = 0, \pm 1, \dots, \pm S - 1$ , and  $\lambda_k = \frac{k\lambda_0}{S}$ ,  $k = 0, \dots, S - 1$  for some  $\lambda_0 > 0$ .

Step 3. Compute  $\widetilde{f}_{-m}(-\lambda)$  by either of the following ways:

*Algorithm 1.* For each  $\lambda$ , let  $[\widehat{\Lambda}_0(\lambda)]$  and  $[\widehat{\mathcal{T}'_\mu f}_m(\lambda)]$  denote the row vectors with their elements given by  $\widehat{\Lambda}_{0n}(\lambda)$  and  $\widehat{\mathcal{T}'_\mu f}_{mn}(\lambda)$ , respectively. For each  $m$ , compute  $\widetilde{f}_{-m}(-\lambda)$  by

$$\widetilde{f}_{-m}(-\lambda) = \frac{[\widehat{\mathcal{T}'_\mu f}_m(\lambda)][\widehat{\Lambda}_0(\lambda)]^T}{[\widehat{\Lambda}_0(\lambda)][\widehat{\Lambda}_0(\lambda)]^T + \sigma}, \quad (15)$$

where  $\sigma$  is a positive constant close to zero.

*Algorithm 2.* For each  $\lambda$ , let  $[\widehat{\Lambda}(\lambda)]$ ,  $[\widehat{\mathcal{T}'_\mu f}(\lambda)]$  and  $[\widehat{f}(\lambda)]$  denote the matrices with their corresponding elements given by  $\delta_m \widehat{\Lambda}_{0n}(\lambda)$ ,  $\widehat{\mathcal{T}'_\mu f}_{mn}(\lambda)$  and  $\delta_m \widetilde{f}_{-n}(-\lambda)$ , where  $m$  and  $n$  denote the row and column numbers, respectively. Then,

$$[\widehat{f}(\lambda)] = [\widehat{\Lambda}(\lambda)] \left( [\widehat{\Lambda}(\lambda)]^T [\widehat{\Lambda}(\lambda)] + \sigma I \right)^{-1} [\widehat{\mathcal{T}'_\mu f}(\lambda)]^T, \quad (16)$$

where  $\sigma$  is a positive constant close to zero. Note that a generalization of *Algorithm 2* for  $\mu = 0$  was presented in our earlier work [11].

Step 4. Using Equation 10, form  $\widehat{f}_{mn}(\lambda)$  and take the inverse  $M(2)$ -Fourier transform to obtain  $f$ .

In step 3,  $\widehat{\Lambda}_{\mu 0n}$  can be very close to zero, making the inverse filtering numerically unstable. Therefore, the inverse filter is replaced with its regularized linear least square version to stabilize the inversion.

A fast implementation of the  $M(2)$ -Fourier transform is implemented as described in [5, 11].

#### 6. NUMERICAL SIMULATIONS

Numerical simulations are performed on a two-dimensional modified Shepp-Logan phantom image of  $13.1 \times 13.1 \text{ cm}^2$ , discretized by  $129 \times 129$  pixels. The  $M(2)$ -Fourier transform was numerically implemented as described above. All numerical implementations were performed using MATLAB. Figure 1 and 2 present the reconstructed images using the proposed algorithms for  $\mu = 0.154 \text{ cm}^{-1}$  and  $\mu = i0.154 \text{ cm}^{-1}$ , respectively. In all reconstructions,  $\sigma$  is set to  $10^{-10}$ . The case for  $\mu = 0$  was studied previously in [11, 12]. These simulations demonstrate the viability of the proposed method and algorithms.

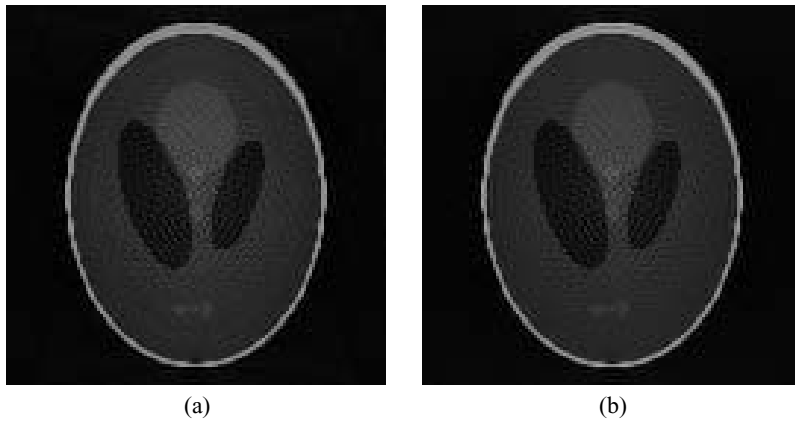


**Fig. 1.** Reconstruction of the modified Shepp-Logan phantom using the proposed algorithms for  $\mu = 0.154\text{cm}^{-1}$ . (a) *Algorithm 1*,  $\sigma = 10^{-10}$ . (b) *Algorithm 2*,  $\sigma = 10^{-10}$ .

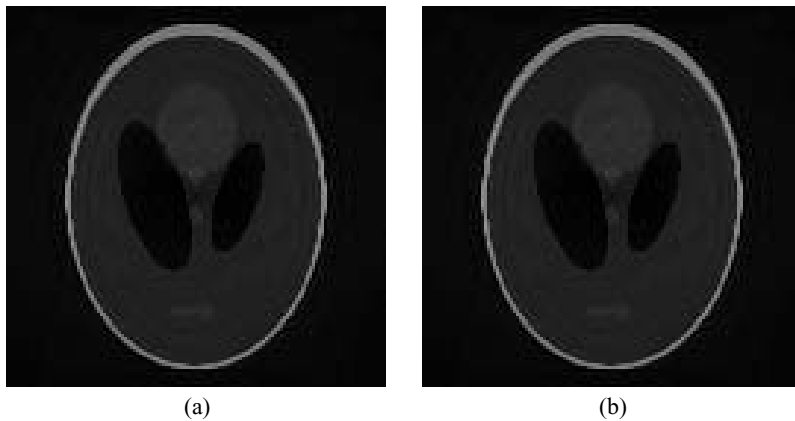


**Fig. 2.** Reconstruction of the modified Shepp-Logan phantom using the proposed algorithms for  $\mu = i0.154\text{cm}^{-1}$ . (a) *Algorithm 1*,  $\sigma = 10^{-10}$ . (b) *Algorithm 2*,  $\sigma = 10^{-10}$ .

## 7. CONCLUSION

In this paper, a block diagonal form of the modified exponential Radon transform in the  $M(2)$ -Fourier domain is derived and a new method of inversion for the exponential Radon transform using the  $M(2)$ -Fourier transform is introduced. Numerically stable algorithms are introduced. Viability of proposed method and algorithms is demonstrated by numerical simulations.

## 8. REFERENCES

- [1] Bellini S, Piancentini M, Cafforio C, Rocca F 1979 *IEEE Transactions on Acoustics, Speech, and Signal Processing ASSP-27* 213–218
- [2] Hawkins G W, Leichner P K, Yang, N-C 1988 *IEEE Transactions on Medical Imaging* 7 135–148
- [3] Inouye T, Kose K, Hasegawa A 1989 *Phys. Med. Biol.* 34 299–304
- [4] Kuchment P, Shneiberg I 1994 *Applicable Analysis* 53 221–231
- [5] Kyatkin A B, Chirikjian G S 2000 *Applied Computational Harmonic Analysis* 9 220–241
- [6] Metz C E, Pan X 1995 *IEEE Transactions on Medical Imaging* 14 643–658
- [7] Natterer F 1986 *The Mathematics of Computerized Tomography* (New York: Wiley-Teubner)
- [8] Puro, A 2001 *Inverse Problems* 17 179–1888
- [9] Tretiak O, Metz C 1980 *SIAM J. Appl. Math.* 39 341–354
- [10] Vilenkin N J 1988 *Special functions and the theory of representations* (Providence: American Mathematical Society)
- [11] C.E. Yarman, B. Yazıcı, “Radon transform inversion via Wiener filtering over the Euclidean motion group,” *Proceedings of IEEE international Conference on Image Processing, vol 2*, Barcelona, Spain, pp. 811–814, 2003.
- [12] C.E. Yarman, B. Yazıcı, 2004 “Radon transform inversion based on harmonic analysis of the motion group,” (preprint)